Mechanical Testing of Ultra-high Temperature Alloys

by R. Völkl and B. Fischer

ABSTRACT—Specially designed facilities for tensile testing of ultra-high temperature alloys are presented. Ohmic heating is chosen for easy access to the sample, fast attainable heating and cooling rates, simplicity in design and operation. Strain is measured with a video extensometer by means of the software SuperCreep. The algorithm for the strain measurements is described. Stability and accuracy of the test system were determined by testing an oxide dispersion strengthened Pt alloy. Performance of the video extensometer was checked by thermal expansion tests on pure Pt. Tensile tests of the oxide dispersion strengthened alloy Pt–10 wt% Rh DPH at 1600°C have proven the reliability of the equipment.

KEY WORDS—Test facility, strain measurement, video extensometer, image analysis, high temperature, platinum, ODS

Introduction

For the development and proper selection of a structural material for application at ultra-high temperatures the mechanical properties have to be known. However, high prices and limited availability of test material along with extremely high testing temperatures make the use of commercial test equipment difficult.

Suitable test equipment has to meet several expectations. Small samples and simple design and operation of the test facility are prerequisites for economical test programs. Furthermore, small specimens enable mechanical testing from the beginning of a development program when only a small amount of material is available. Strain measurement at ultra-high temperatures has to be performed without affecting the mechanical behavior of the small samples. The absolute temperature as well as the temperature distribution over the gage length has to be controlled for the testing time.

Axial extensometers use extension rods to separate the strain sensor from the hot specimen. Reppich et al.[1] and Schmidt[2] used an inductive linear position transducer with Al_2O_3 extension rods for tension tests at temperatures of up to 1400°C. However, problems may arise at ultra-high temperatures because even small contact forces can lead to considerable stress concentrations in a small specimen. The maximum, long-term operational temperature in air of the usual ceramic extension rods is around 1500°C. For higher temperatures, water-cooling and precise mounting requirements make their use complicated.

R. Völkl (rainer.volkl@uni.bayreuth.de) is a Senior Researcher, University of Bayreuth, Metallic Materials, Ludwig-Thoma Straße, 366, D-95440, Germany. B. Fischer is a Professor, University of Applied Sciences, Jena, Germany.

Original manuscript submitted: March 6, 2002.
Final manuscript received: November 13, 2002.
DOI: 10.1177/0014485104042451

Noncontacting strain-measurement techniques overcome these problems. A simple approach is to remove the strain-measuring device from the hot zone and measure the displacement of the load assembly instead. Hamada et al.[3] used this method for creep measurements on Pt alloys at temperatures up to 1500°C. They determined the elongation of the sample by measuring the displacement of the pull rod ends with the aid of a laser extensometer. However, the compliance of the whole system has to be known to extract the true strain using these techniques. Ho and MacEwen[4] also used a so-called remote extensometer attached to shoulders at both ends of a tension specimen which jut out of the furnace. The extensometer was made of Invar in order to minimize thermal expansion. Ho and MacEwen[4] assumed that once the specimen goes into plastic flow, the overall elongation results primarily from elongation within the smaller gage section of the specimen inside the furnace and true strain could be calculated.

Other noncontacting approaches for strain measurement at high temperatures use computer vision techniques, laser Doppler or laser speckle techniques. Gaudig et al.[5] measured the lateral strain in the necked region of creep samples by means of digital image processing. They could achieve an accuracy of 0.25 pixels, which corresponds to a displacement of ± 0.01 mm or ± 0.01 true strain at temperatures lower than 850°C.

The digital image correlation (DIC) methods are based on specimens with randomly distributed speckles at the surface. Lyons et al.[6] coated nickel-based alloys with BN or Al_2O_3 scales in order to create black speckles on a white surface. By correlating subsequent digital images of the specimens they could determine the complete elastic and thermal surface displacement field up to 700°C. Maximum strains of 8×10^{-2} and 2×10^{-2} were recorded during thermal expansion and tension tests. Lyons et al.[6] reported an accuracy of the order of 10^{-3} for their strain measurement system. At temperatures above about 700°C, illumination problems due to increasing self-radiation of the specimen often arise with DIC. Decorrelation effects can be introduced by image distortion caused by a furnace window or variations in the refractive index of the heated atmosphere. Large strains and surface oxidation may also disturb the surface speckle pattern.

Anwander et al.[7] circumvented illumination problems by combining DIC with two laser diode beams, each having a diameter of ≈3 mm. With a suitable choice of filters or an electronic shutter the reflected laser light can outweigh the thermal radiation of the specimen even at 1600°C (λ = 668 nm, maximum output power of laser diodes 15 mW). The displacements of the surface elements cause movements of the

speckle patterns. The difference of the surface displacements divided by the distance between the two illuminated surfaces areas gives the strain. The digital laser speckle extensometer proved reliability for measurements of thermal and mechanical strains up to 1200°C. Decorrelation effects could be minimized by using two independent illumination and image capture systems. Various sample geometries can be employed and no special surface preparation is needed.

Single- and multi-zone furnaces in conjunction with thermocouples and PID controllers are common for heating and temperature control. Whether the grips are placed inside or outside the furnace different materials are possible. Reppich et al.[1] and Schmidt[2] introduced the specimen along with the grips into a high-temperature single-zone furnace. For measurements at temperatures of up to 1400°C, Al_2O_3 was chosen for the grips. In the creep test facility of Hamada et al.,[3] the grips also experienced high temperatures of up to 1500°C in a single-zone furnace. For that reason, Hamada et al.[3] utilized an extremely expensive ODS platinum alloy for making the grips. To minimize cost, small specimens were used and the load applied from outside the furnace via a bar linkage.

Stainless steels or other common materials can be used if the grips are placed outside the furnace, but it becomes increasingly difficult to maintain a negligible temperature gradient over the gage length. Ho and MacEwen[4] surmounted this difficulty with a miniature three-zone furnace.

Induction heating is often a better choice than a radiation furnace system if fast heating and cooling rates are of interest. Petersen and Rubiolo[8] opted for ohmic heating because of easy access of the gage length of the sample for temperature and strain measurement, and because of the simplicity in design and operation.

Principles

Design of Test Facilities

The interest of the current research is on metallic materials for ultra-high temperature applications. The test temperatures of interest range from 1000°C for Pt/Au alloys, up to 3000°C for Re/W alloys.[9] Special test facilities[10–12] were designed and built at the University of Applied Sciences Jena. A schematic diagram of the test facilities is given in Fig. 1.

A gas-tight specimen chamber is mounted in a commercial servomotor driven test machine. The chamber permits tests either in air or in a protective gas atmosphere. Ohmic heating of the sample leads to lower temperatures at the grips rather than in the center of the specimen; consequently, cheaper copper grips can be used. Ohmic heating was also chosen for easy access to the sample, fast attainable heating and cooling rates and simplicity in design and operation. A steel pull rod is connected with the load cell at the crosshead of the test machine. Strips with typical dimensions of $120 \times 4 \times 1$ mm^3 or thin wires are tested. All functions are computer controlled with the software LabView and SuperCreep,[12] developed by the authors for strain measurements by means of digital image analysis. A PID controller realized with LabView regulates the 0–10 V analog input of a thyristor, which is connected to the primary side of a 100 kVA transformer. The secondary side of the transformer heats the specimens with 50 Hz alternating current in short circuit.

The temperature is measured in the range of 750–3000°C with a pyrometer operating at wavelengths of 0.7–1.1 μm and an operating distance of 250 mm. The measurement area

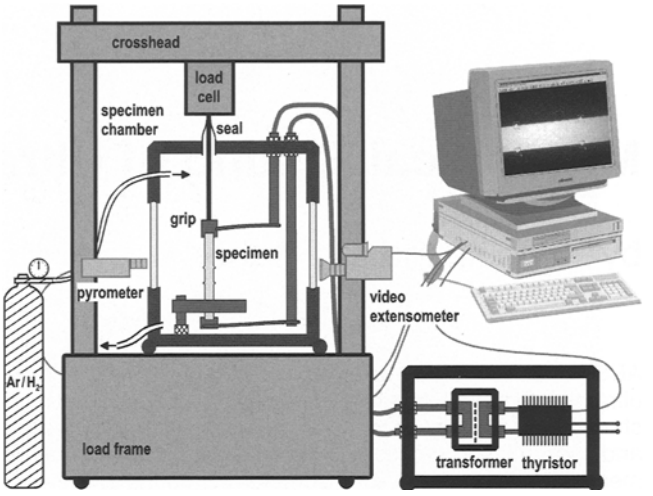

Fig. 1—Schematic diagram of the equipment used to measure mechanical properties of metals at temperatures up to 3000°C

at the sample has a diameter of approximately 0.5 mm. Fast, built-in scan and maximum value storage features enable safe detection of the maximum temperature in a rectangular area of 18×0.5 mm^2 on the specimen surface. An accuracy of 0.3% and an adjustable response time down to 1 ms guarantee secure temperature control even at high heating rates.

For precise temperature measurements, the spectral emissivity of the investigated material has to be known as a function of temperature and wavelength. Problems may arise during long-time exposure at high temperature due to oxidation or other types of surface changes. Neuer et al.[13,14] measured the total and spectral emissivity of various Pt/Rh alloys up to 1350°C. Pt/Rh alloys show generally very slow oxidation. Above about 1000°C the oxide scales evaporate. Neuer et al.[13] therefore recommend Pt/Rh alloys as reference materials. Calibration of the test system for materials with unknown emissivity can be performed with a thin foil of a Pt/Rh alloy attached to the specimen. Assuming good thermal contact, the emissivity of the material is determined by comparing the indicated temperature when the pyrometer is first focused on the Pt/Rh foil and then on the specimen just beside the foil.

Hardware

Strain is measured with the noncontacting video extensometer SuperCreep. The video extensometer consists of a Peltier cooled 2/3 inch charge-coupled device (CCD) camera SensiCam,[15] with 1280×1024 pixel resolution and 12-bit dynamic resolution. A variable exposure time from 1–1000 ms allows us to grab images up to 2000°C without introducing filters in the optical path. Telecentric lenses minimize perspective distortions caused by a variable object distance.

SuperCreep controls the camera and the frame grabber. Due to ohmic heating only the central part of the sample sees high temperatures. As a consequence, strain has to be measured in this central zone, where the plastic deformation is concentrated. The problem is resolved by markers on the specimen in the central zone. SuperCreep continuously determines the distances between corresponding markers.

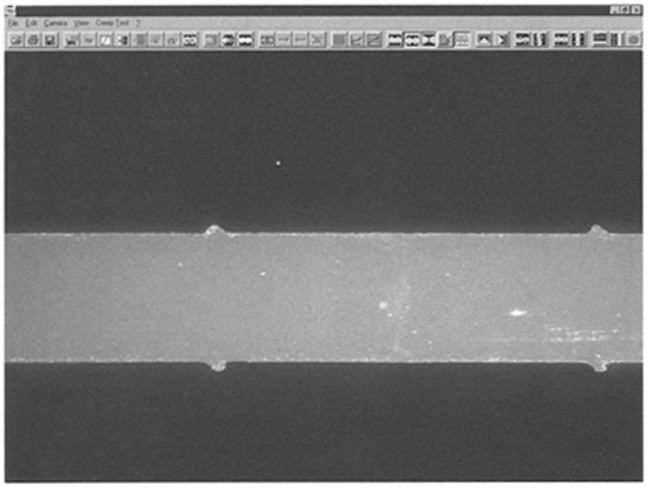

Fig. 2—Image of self-radiating Pt–10% Rh DPH specimen at 1500°C. The sample is laser cut out of a sheet with four small shoulders. The initial gage length defined by two corresponding markers is 10 mm

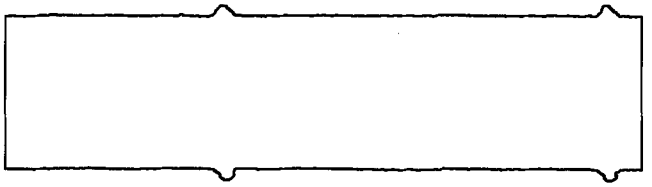

Fig. 3—Contour of a specimen

Suitable markers for high-temperature tests can be made by laser cutting samples with small shoulders from sheet material. This technique was successfully applied on Pt–10% Rh DPH (Fig. 2). The ODS alloy Pt–10% Rh DPH was developed by W.C. Heraeus GmbH & Co. KG, Hanau, Germany in cooperation with the University of Applied Sciences Jena.[16–18]

Algorithm for Strain Measurement

A two-step approach is implemented in SuperCreep in order to guarantee fast and precise strain measurements with the aid of computer vision techniques.

As a first step, the algorithm detects the approximate positions of the markers on the contour of the specimen. A copy of the specimen image, Fig. 2, is converted into a binary image and subsequently the contour, Fig. 3, is coded according to the procedure by Freeman.[19] The Freeman[19] chain code

$$C = c_1,\ c_2,\ \ldots,\ c_n, \tag{1}$$

of the specimen contour leads to further data reduction and facilitates marker detection.

The Freeman[19] chain code is based on the pixel grid of a digital image. Eight directions between adjoining pixels are distinguished (Fig. 4). The coordinates of the starting point of the contour, together with a list of the coded directions,

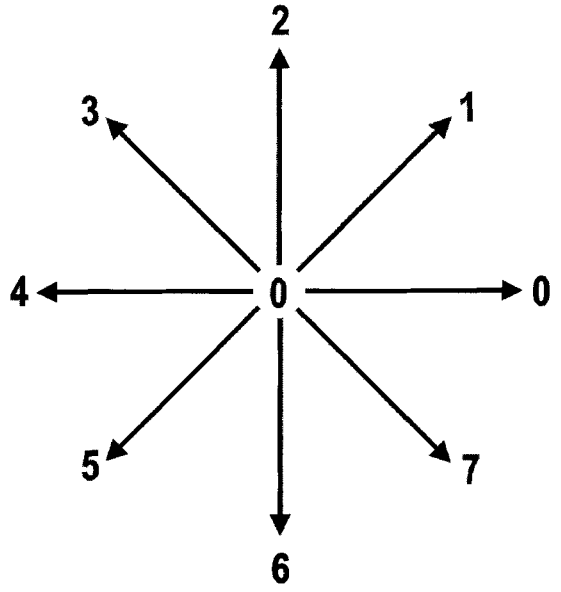

Fig. 4—Coding of the direction of a contour segment with an eight-neighbor code according to Freeman[19]

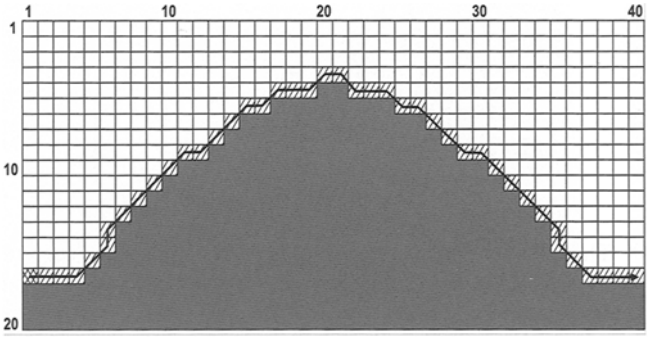

Fig. 5—The marker contour pattern is correlated with the sample contour in order to detect the marker positions

completely determine the image feature. In the same way as the specimen outline, the marker contour pattern (Fig. 5) is represented by the chain code

$$P = p_1,\ p_2,\ \ldots,\ p_m \tag{2}$$

and the start point M_P. For the contour pattern example in Fig. 5, the chain code P is given by

$$P = 0, 0, 0, 1, 1, 2,\ \ldots, 6, 7, 7, 0, 0, 0$$

and the start point M_P by

$$M_P = (1,\ 17).$$

The resemblance between a segment of the specimen contour at the position j and the contour of the marker pattern is quantified with the chain cross-correlation function[20] $k(j)_{C,P}$ of the two chain codes C and P:

$$k(j)_{C,P} = \frac{1}{m}\sum_{i=1}^{m}\cos\left((c_{j+i} - p_i)\frac{\pi}{4}\right). \quad (3)$$

The chain cross-correlation function becomes 1 if a segment of the specimen contour matches the marker contour pattern exactly. If the contours are rotated by 180° with respect to each other, $k(j)_{C,P}$ becomes –1. If a segment of the specimen contour is rotated by 90° or –90° the chain cross-correlation function equals 0. Rough positions of the four markers are detected by searching two maxima and two minima of the function $k(j)_{C,P}$.

In order to reach subpixel accuracy the complete 12-bit gray-level information of the CCD camera is evaluated in small regions centered at the coordinates of the maxima and minima. The regions are first stored in intermediate images and then processed with 5 × 5 gradient convolution masks[21] (eqs (4) and (5)) in order to approximate the brightness gradient between the sample and the background:

$$\nabla_x = \begin{pmatrix} -10 & -10 & 0 & 10 & 10 \\ -17 & -17 & 0 & 17 & 17 \\ -20 & -20 & 0 & 20 & 20 \\ -17 & -17 & 0 & 17 & 17 \\ -10 & -10 & 0 & 10 & 10 \end{pmatrix} \quad (4)$$

$$\nabla_y = \begin{pmatrix} 10 & 17 & 20 & 17 & 10 \\ 10 & 17 & 20 & 17 & 10 \\ 0 & 0 & 0 & 0 & 0 \\ -10 & -17 & -20 & -17 & -10 \\ -10 & -17 & -20 & -17 & -10 \end{pmatrix}. \quad (5)$$

The upper-left shoulder of the sample in Fig. 2 is processed as an example. Figure 6 represents the absolute values of the gradient in the x- and y-directions. Bright shading indicates a high gradient. The highest absolute value of the gradient is considered to fix the edge of the sample. The precise shoulder position in the x-direction is assigned to the x-coordinate of the center of gravity of the x-gradient image. In the same manner, the precise shoulder position in the y-direction is assigned to the y-coordinate of the center of gravity of the y-gradient image. The white lines in Fig. 6 indicate the x- and y-coordinates of the precise shoulder position.

The practice shows that the measurements become almost independent of the illumination, i.e., the brightness, if gradients are considered instead of the image gray-level itself. The algorithm is robust so that even thin wires wound around the specimen can serve as markers.

Experimental Details

Test Procedure

A typical tension test consists of the following steps:

- grip the specimen;
- start the video extensometer;
- heat the specimen to the desired temperature;
- start the constant strain rate tension test.

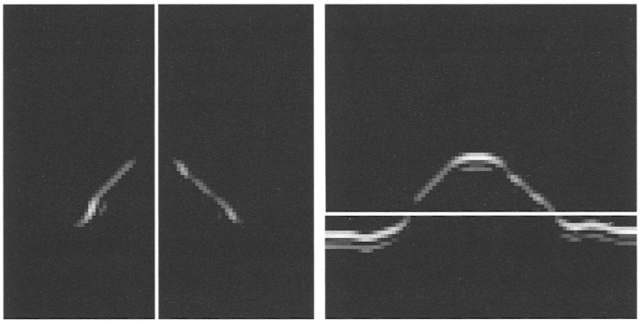

Fig. 6—Images of the absolute gradients in the x-direction (left) and the y-direction (right) at the upper-left shoulder in Fig. 2

Alternatively, constant-stress creep tests can be performed in order to determine stress rupture data and creep properties.[22]

Performance

The temperature distribution on a 100 mm long sample of the alloy Pt–10% Rh DPH[16–18] was measured with a calibrated pyrometer. The specimen was heated to 1500°C at the center. In a zone of 30 mm around the center, the temperature could be controlled with accuracy of 1500 ± 5°C and in a zone of 10 mm between the markers the temperature could be controlled within 1500 ± 2°C. During a subsequent constant-stress creep test, the temperature between the markers could be held constant within 1500 ± 3°C until necking occurred. Due to the ohmic heating, the temperature outside the necked region is always lower, whereas in the necked region the temperature is kept at the desired value.

The test facility allows fast heating and cooling cycles. In another test on Pt–10% Rh DPH a maximum temperature of 1506°C was reached within 12 s. After 15 s, the maximum temperature was constant at 1500 ± 2°C. After switching the power off, the specimen took about 20 s to cool down to 750°C. Heating rates of 100°C s^{-1} and cooling rates of 30°C s^{-1} can be achieved in routine application.

The accuracy of the video extensometer was checked by repeated measurements of the initial gage length l_0 of a Pt–10% Rh DPH specimen heated to 1500°C without an applied load (Fig. 2). Strain was calculated according to

$$\varepsilon = \frac{l - l_0}{l_0} \quad (6)$$

where ε is the engineering strain, l_0 is the initial gage length, and l is the actual distance between the markers.

Provided that the distance between the markers is always determined with the same accuracy, Δl, eq (7) gives the error of a single strain measurement

$$\Delta\varepsilon = \left|\frac{l - l_0}{l_0^2} + \frac{2}{l_0}\right|\Delta l \quad (7)$$

where $\Delta\varepsilon$ is the error of a single strain measurement, Δl is the accuracy of a single distance measurement, l_0 is the initial gage length, and l is the actual distance between the markers.

The telecentric lens used for this investigation had a magnification of 0.5 and a telecentric range of 12 mm at a working

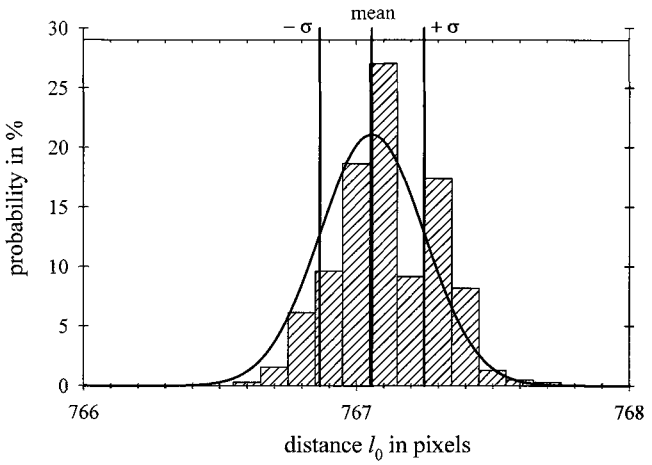

Fig. 7—Statistics over 600 measurements on a Pt–10% Rh DPH specimen heated to 1500°C without an applied load

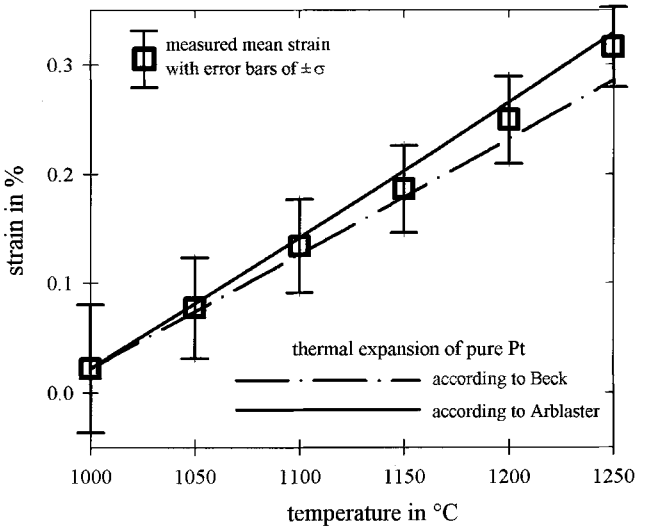

Fig. 8—Measured thermal strain of pure Pt compared to literature data according to Beck[23] and Arblaster[24]

distance of 115 mm. Thus, an object of 10 mm diameter has an image size of 5 mm. Consequently, the object distance between the markers of about 10 mm (Fig. 2) results in an image distance of about 5 mm or 730 pixels on the 2/3 inch (8.8 × 6.6 mm^2) 1280 × 1024 CCD chip.

In order to determine the error of a single distance measurement, a Pt–10% Rh DPH specimen (see Fig. 2) was heated to 1500°C without an applied load. Six hundred measurements were recorded with an acquisition rate of 1 Hz. No systematic shift was observed during the testing time. The mean value over 600 measurements was l_0 = 767.0 pixels with a standard deviation of Δl = 0.2 pixels (Fig. 7).

All markers have to remain in the field of view during the test for a correct strain measurement. This means the image distance on the CCD chip may not exceed l = 1280 pixels during a tensile test. So, the maximum measurable strain is about $\varepsilon \approx 60\%$, if an initial gage length of about $l_0 \approx 770$ pixels is assumed. Introducing l = 1280 pixels, l_0 = 767.0 pixels and Δl = 0.2 pixels into eq (7) a maximum error $\Delta\varepsilon \approx \pm 0.07\%$ or 700 microstrains is calculated. The reproducibility is better than 0.25% of full-range output.

The accuracy can be improved by increasing the initial distance l_0 between the markers. However, the maximum measurable strain would decrease. A 400 MHz personal computer allows strain measurements with a rate of about 5 Hz. If slower measurement rates are sufficient the error $\Delta\bar{\varepsilon}$ of the mean can further be decreased by mean filtering over n single measurements according to

$$\Delta\bar{\varepsilon} = \frac{\Delta\varepsilon}{\sqrt{n}}. \tag{8}$$

To verify the performance of the video extensometer we studied the thermal expansion of pure Pt at temperatures above 1000°C. Pure Pt was chosen because precise thermal expansion data are available from Beck[23] and Arblaster.[24] The smallest possible load of about 1.4 MPa was applied to the Pt sample (120 × 4 × 1 mm^3). The load was due to the weight of the electric current connector. The temperature was increased in steps of 50°C each from 1000°C up to 1250°C. Temperatures higher than 1250°C were not attempted in order to avoid pronounced creep strain during the test time. Two to three hundred measurements were taken at each temperature. The standard deviations $\sigma_\varepsilon = \pm(0.04\text{–}0.05)\%$, given in Fig. 8, are in good agreement with the previously calculated error of $\Delta\varepsilon \approx \pm 0.07\%$. Figure 8 shows that the measured mean thermal strains were consistently between the values reported by Beck[23] and Arblaster.[24]

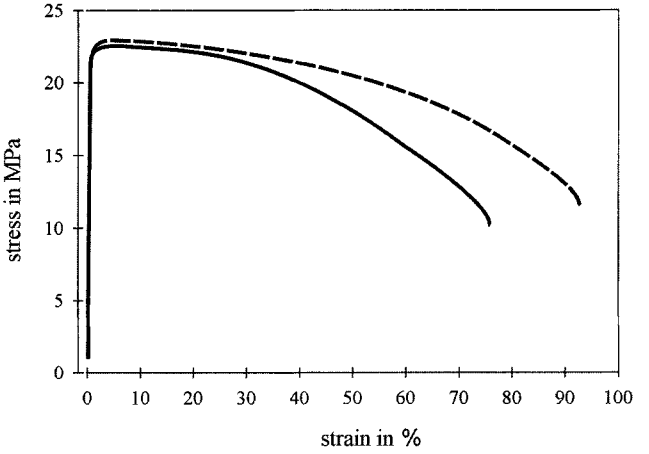

Fig. 9—Tensile stress–strain curves of Pt–10% Rh DPH at 1600°C

Tension Test Results

Tensile stress–strain curves of Pt–10% Rh DPH were determined at 1600°C in air (Fig. 9). The experiments were performed with a strain rate of 1.7 × 10^{-3}s^{-1}. In order to measure plastic strains of up to 150% a telecentric lens with a magnification of 0.33 was used instead of the lens with magnification of 0.5 mentioned above. In the first test, a yield strength of 21.8 MPa, an ultimate tensile strength of 22.7 MPa and a fracture strain of 76% were determined. In the second test, a yield strength of 21.8 MPa, an ultimate tensile strength of 22.9 MPa and a fracture strain of 93% were determined.

Conclusions

Test facilities for tension tests on conducting materials at ultra-high temperatures have been described. Ohmic heating allows fast heating rates up to ultra-high temperatures and easy temperature control by an infrared pyrometer. The grips do not see high temperatures, hence a cheaper copper alloy can be used. With carefully chosen specimen geometry the detrimental effects of temperature gradients due to ohmic heating can be minimized. Optical access to the sample facilitates strain measurement by means of digital image processing.

A measurement error of $\pm$ 0.2 pixels at the camera sensor results in a strain resolution better than 700 microstrains (0.25% of full-range output). The typical accuracy of $\pm$ 0.02 pixels reported by Lyons et al.[6] for digital image correlation techniques at ambient temperature could not be reached. However, the chosen approach is not susceptible to decorrelation effects and allows real-time strain measurements with a rate of at least 5 Hz.

The digital laser speckle correlation techniques have a potential for very precise strain measurements even at high temperatures. To reduce the influence of thermal radiation, filters have to be inserted into the optical path to detect reflected laser light only. Anwander et al.[7] report an uncertainty of about 50 microstrains and a quantization error of 20 microstrains for strain measurements with their laser speckle extensometer at temperatures of up to 1200°C. To overcome decorrelation effects due to plastic deformation and other effects, Anwander et al.[7] use a repetitive reinitialization of the image acquisition system. They calculate total strain by accumulating strain increments determined between successive pairs of grabbed images. This strain accumulation approach is likely to lessen accuracy due to error propagation. However, the high accuracy of digital laser speckle correlation techniques goes together with high equipment cost.

The tension test facilities with video extensometers have been used successfully during numerous test programs. Tests on γ-TiAl, Mo-based, Re-based,[9] Pt-based solid solution and/or oxide dispersion hardened alloys,[17, 25–28] Pt-based refractory superalloys[29] and metallic Ir[30] were performed at temperatures ranging from 700 to 3000°C. Low costs and easy operation are in practice often more important than highest accuracy.

Noncontacting strain and temperature measurement methods enable the use of small specimens. Low cost, small sample size and fast feedback are prerequisites for a test scheme to be used in the early steps of an alloy development program. The development and characterization of the abovementioned DPH materials within five years was only possible by optimizing strength and ductility from the very beginning of the project through extensive mechanical tests.

Acknowledgments

The authors would like to thank the Carl Zeiss Foundation for financial support in the development of the video extensometer and W. C. Heraeus GmbH & Co. KG for the Pt alloys.

References

1. Reppich, B., Brungs, F., Hümmer, G., and Schmidt, H., "Modelling of the Creep Behaviour of ODS Platinum-Based Alloys," in Proceedings of the 4th International Conference on Creep and Fracture of Engineering Materials and Structures, R.W. Evans and B. Wilshire, eds, The Institute of Metals, Swansea, UK, 142–158 (1990).

2. Schmidt, H., "Dispersionshärtung in Platin und Platinlegierungen" ("Dispersion Strengthening of Platinum and Platinum Alloys"), Doctoral thesis, Erlangen (1986).

*3. Hamada, T., Hitomi, S., Ikematsu, Y., and Nasu, S., "High-Temperature Creep of Pure Platinum," Materials Transactions, JIM, **37** (3), 353–358 (1996).*

*4. Ho, E.T.C. and MacEwen, S.R., "A Facility for Precise Measurement of Mechanical Properties at Elevated temperatures," Journal of Metals, **35** (2) 25–28 (1983).*

*5. Gaudig, W., Bothe, K., Bhaduri, A.K., and Maile, K., "Determination of the Geometric Profile and Stress/Strain State in the Necked Region During Inelastic Deformation at Elevated Temperatures Using a Non-Contacting Measurement Technique," Journal of Testing and Evaluation, **24** (3), 161–167 (1996).*

*6. Lyons, J.S., Liu, J., and Sutton, M.A., "High-Temperature Deformation Measurements Using Digital-Image Correlation," EXPERIMENTAL MECHANICS, **36** (1), 64–70 (1996).*

*7. Anwander, M., Zagar, B.G, Weiss, B., and Weiss, H., "Non-Contacting Strain Measurements at High Temperatures by the Digital Laser Speckle Technique," EXPERIMENTAL MECHANICS, **40** (1), 98–105 (2000).*

*8. Petersen, C. and Rubiolo, G.H., "High-Temperature Thermal Fatigue of AISI 316L Steel," Journal of Nuclear Materials, **179**, 488–491 (1991).*

9. Fischer, B., Freund, D., and Lupton, D.F., "Stress-Rupture Strength of Rhenium at Very High Temperatures," in Proceedings of the International Symposium on Rhenium and Rhenium Alloys, TMS Annual Meeting, Orlando, FL, 311–320 (1997).

10. Fischer, B., Helmich, R., and Töpfer, H., "Anordnung zur Warmfestigkeitsprüfung hochschmelzender, elektrisch leitender Werkstoffe" ("Equipment to Measure the Hot Strength of High Melting Point, Electric Conductive Materials"), DD Patent 245576 A3 (1982).

*11. Fischer, B., Töpfer, H., and Helmich, R., "Gerät für Warmfestigkeitsmessungen an hochschmelzenden Metallen nach Einwirkung silikatischer Schmelzen" ("Facility to Measure the Hot Strength of High Melting Point Metals After Exposure to Silica Glass Melts"), Silikattechnik, **35** (11), 329–331 (1984).*

12. Völkl, R., Freund, D., Fischer, B., and Gohlke, D., "Berührungslose Dehnungsaufnahme an widerstandsbeheizten Metallzugproben mit Hilfe digitaler Bildverarbeitung bei Prüftemperaturen bis 3000°C" ("Non-Contacting Strain-Measurement on Ohmic Heated Metallic Tension Test Samples With the Aid of Digital Image Processing at Temperatures of up to 3000°C"), in Proceedings of the Conference Werkstoffprüfung 1998, Bad Nauheim, Germany, Deutscher Verband für Materialforschung und -prüfung e.V., Berlin, Germany, Werkstoffprüfung Berichtsbände, No. 638, 211–218 (1998).

13. Neuer, G., Pohlmann, P., and Schreiber, E., "Gesamtemissionsgrad und spektraler Emissionsgrad von Hochtemperaturmaterialien" ("Total Emissivity and Spectral Emissivity of High Temperature Materials"), Technical Report IKE 5-249, Stuttgart (1998).

*14. Neuer, G. and Jaroma-Weiland, G., "Spectral and Total Emissivity of High Temperature Materials," International Journal of Thermophysics, **19** (3), 917–929 (1998).*

15. PCO Computer Optics GmbH, Donaupark 11, D-93309 Kelheim, Germany, http://www.pco.de/.

16. Fischer, B., Goy, k.-H., Kock, W., Lupton, D. F., Manhardt, H., Merker, J., Schölz, F., and Zurowski, B., "Dispersionsverfestigter Platin-Werkstoff, Verfahren zu seiner Herstellung und seine Verwendung" ("Dispersion Strengthened Platinum Material, Manufacture Route and Application"), DE Patent 197 14 365 A1 (1998).

17. Völkl, R., Glatzel, U., Broemel, T., Freund, D, Fischer, B., and Lupton, D., "Creep of Platinum Alloys at Extremely High Temperatures," in Proceedings of the 9th International Conference of Creep and Fracture of Engineering Materials and Structures, J.D. Parker, ed., The Institute of Materials, 21–27 (2001).

*18. Fischer, B., "New Platinum Materials for High Temperature Applications," Advanced Engineering Materials, **3** (10), 811–820 (2001).*

*19. Freeman, H., "Computer Processing of Line Drawing Images," Computing Surveys, **6** (1), 57–97 (1974).*

20. Schmid, R., "Industrielle Bildverarbeitung" ("Industrial Image Processing"), W. Schneider, ed., Vieweg, Wiesbaden (1995).

21. Bässmann, H. and Besslich, P.W., "Image Processing Ad Oculos," DBS GmbH, Bremen, Germany (1993).

*22. Völkl, R., Freund, D., and Fischer, B., "Economic Creep Testing of Ultra-High Temperature Alloys," Journal of Testing and Evaluation, **31** (1), 35–43 (2003).*

23. Beck, G., "Edelmetall-Taschenbuch" ("Precious Metals Handbook"), A.G. Degussa, ed., Hüthig, Heidelberg (1995).

24. Arblaster, J.W., "Crystallographic Properties of Platinum," Platinum Metals Review, **41** *(1), 12–21 (1997).*

25. Fischer, B., Freund, D., Brömel, T., Völkl, R., Daniel, J., Ross, W., Teschner, R., and Michelsen, C.-E., "Practical Experience With New Oxide Dispersion Hardened Platinum Materials," in Proceedings of the 25th International Precious Metals Conference, Tuscon, AZ International Precious Metals Institute, Pensacola, FL (2001).

26. Völkl, R., Freund, D., Fischer, B., and Gohlke, D., "Comparison of the Creep and Fracture Behaviour of Non-Hardened and Oxide Dispersion Hardened Platinum Base Alloys at Temperatures Between 1200°C and 1700°C," in Proceedings of the 8th International Conference of Creep and Fracture of Engineering Materials and Structures, Key Engineering Materials Vols. 171–174, Trans. Tech Publication, Tsukuba, Japan, 77–84 (1999).

27. Fischer, B., Behrends, A., Freund, D., Lupton, D., and Merker, J., "Dispersion Hardened Platinum Materials for Extreme Conditions," in Proceedings of The Minerals, Metals and Materials Society (TMS) Annual Meeting 1999, San Diego, CA, 321–331 (1999).

28. Lupton, D.F., Merker, J., Fischer, B., and Völkl, R., "Platinum Materials for the Glass Industry," in Proceedings of the 24th International Precious Metals Conference 2000, Williamsburg, VA, International Precious Metals Institute, Pensacola, FL (2000).

29. Süss, R., Freund, D., Völkl, R., Fischer, B., Hill, P. J., Ellis, P., and Wolff, I.M., "The Creep Behaviour of Pt-base γ/γ Analogues to Ni-Base Superalloys at 1300°C," Materials Science and Engineering A, **338**, *133–141 (2002).*

30. Fischer, B., Lupton, D.F., Braun, F., Merker, J., and Helmich, R., "Zeitstandfestigkeit von Iridium bei extrem hohen Temperaturen" ("Stress-Rupture Strength of Iridium at Extremely High Temperatures"), in Proceedings of the Werkstoffprüfung 1994, Werkstoffprüfung Berichtsbände, Bad Nauheim, No. 634, 141–145 (1994).